A comparative study of the response of buried pipes under static and moving loads

Alzabeebee, Saif; Chapman, David; Faramarzi, Asaad

DOI:
10.1016/j.trgeo.2018.03.001

Document Version
Peer reviewed version

Citation for published version (Harvard):
Alzabeebee, S, Chapman, D & Faramarzi, A 2018, 'A comparative study of the response of buried pipes under static and moving loads', *Transportation Geotechnics*, vol. 15, pp. 39-46.
https://doi.org/10.1016/j.trgeo.2018.03.001

A comparative study of the response of buried pipes under static and moving loads

Saif Alzabeebee (Corresponding author)

Department of Civil Engineering, School of Engineering, University of Birmingham, Birmingham, B15 2TT, UK

E-mail: Saif.Alzabeebee@gmail.com

David N Chapman

Department of Civil Engineering, School of Engineering, University of Birmingham, Birmingham, B15 2TT, UK

E-mail: D.N.Chapman@bham.ac.uk

Asaad Faramarzi

Department of Civil Engineering, School of Engineering, University of Birmingham, Birmingham, B15 2TT, UK

E-mail: A.Faramarzi@bham.ac.uk

Abstract

The buried pipes should be designed properly to withstand the loads imposed by the backfill soil weight and traffic loads. However, a thorough literature review has shown differing opinions on the effect of static and moving traffic loads on buried pipes. Some studies have shown that moving loads produce higher displacement in buried pipes compared to static loads, while other studies have shown contradicting results. These differing opinions have created confusion among researchers who are studying the response of buried pipes under traffic loads, where most of the studies have been conducted using either static or moving loads without proper justification to the selection of the loading type. To clarify this confusion, this paper presents a rigorous study on the behaviour of buried pipes under static and moving traffic loads using a robust finite element analysis. The static and dynamic finite element models have been developed and validated using high-quality field data collected from the literature. The developed models were then used to investigate the effect of the truck speed, pipe stiffness and loading conditions on the maximum displacement of buried pipes. The results showed that the displacement of buried pipes due to static loads is always higher than the pipe displacement due to moving loads. In addition, it was found that the ratio of the static to dynamic pipe displacement decreases as the pipe stiffness increases and increases to a lesser extent as the truck speed increases. Hence, future studies should consider the static loads in designs as these are the most stringent loading condition. This is actually very helpful for designers if they are using numerical methods in their designs, because static analyses are much more straightforward to conduct and less computationally demanding compared to dynamic analyses.

Keywords: moving traffic loads; static traffic loads; buried structures; soil-structure interaction.

1. Introduction

Nowadays, pipelines can be considered as one of the most vital infrastructures in maintaining modern life as they provide a convenient way to transport products such as gas, oil, drinking water, sewage and storm water (Zhou et al., 2017; Khemis et al., 2016; Tee et al., 2013). Pipelines can also be used as economical and safe conduits for electricity and telecommunication lines (Moser and Folkman, 2008). These pipelines are usually buried in the ground to protect them from damage due to natural hazards and/or vandalism. As a result of burying a pipe in the ground, during their service life pipelines need to resist external forces from the soil overburden pressure and traffic loads, if buried below transportation routes and buried at shallow depths. Therefore, buried pipes need to be designed properly to withstand these forces. However, a thorough literature review has shown differing opinions with respect to the effect of static and moving traffic loads (Alzabeebee, 2017). The results from research conducted on large elliptical and box culverts published by Beben (2013) and Acharya et al. (2016) have shown that moving traffic loads produced higher displacement in buried culverts compared to static traffic loads, while other studies have shown contradictory results (Yeau et al., 2009; Sheldon et al., 2015).

Yeau et al. (2009) investigated the performance of in-service corrugated steel elliptical culverts under static and moving truck loads. A total number of 39 in-service culverts were considered in the study. Two trucks were used in these tests. The first truck had a total weight of 302 kN with a maximum axle load of 142 kN. The second truck had a total load of 280 kN with a maximum axle load of 76 kN. Yeau et al. (2009) found that the maximum culvert displacement due to the moving truck loads was 10% to 30% lower than the maximum displacement due to the static truck loads.

Beben (2013) investigated the response of in-service corrugated steel plate elliptical culverts subjected to static and moving truck loads. Four trucks were used in the test with a total weight of 279 kN, 275 kN, 285 kN and 280 kN. The maximum culvert displacement and strain were recorded in each test. The speed of the trucks ranged from 10 km/hr to 70 km/hr. Bebn (2013) found that the maximum displacement and strain induced by the moving truck loads were higher than the corresponding

displacement and strain due to static truck loads. The ratio of the dynamic to static displacement ranged from 1.116 to 1.260, while the ratio of the dynamic to static strain ranged from 1.105 to 1.293.

Sheldon et al. (2015) studied the displacement and the joint rotation of an in-service buried metal pipe due to static and moving truck loads using field based studies. The moving truck tests were conducted with four different truck speeds (8 km/hr, 16 km/hr, 32 km/hr and 48 km/hr). The test truck had a maximum axle load of 133 kN. The results showed that the buried pipe experienced higher displacement due to the static truck loads compared to the corresponding displacement due to the moving truck loads.

Acharya et al. (2016) conducted field studies to investigate the behaviour of buried rigid box culvert under both static and moving loads. The box culvert buried with a backfill height of 0.65 m. The static and moving loads were applied using a low loader truck loaded with a backhoe. The truck had a maximum axle load of 105 kN. The speed of the truck ranged between 40 km/hr to105 km/hr. Acharya et al. (2016) found that the culvert displacement due to the moving load was higher than the static culvert displacement. They also found an increase in the culvert displacement as the truck speed increased.

On the other hand, most of the studies on the behaviour and the design of buried pipes have been conducted using either static loads (Katona, 1990; Arockiasamy et al. 2006; Petersen et al., 2010; Talesnick et al., 2011; Kang et al., 2014; Lay and Brachman, 2014; Rakitin and Xu, 2014; Chaallal et al., 2015a, b; MacDougall et al., 2016; Mohamedzein and Al-Aghbari 2016; Alzabeebee et al., 2017, 2018a) or moving loads (McGrath et al., 2002; Li et al., 2017; Neya et al., 2017) without a rigorous justification with regard to the selection of the loading type. Katona (1990), Arockiasamy et al. (2006), Petersen et al. (2010), Talesnick et al. (2011), Kang et al. (2014), Chaallal et al. (2015a, b), Mohamedzein and Al-Aghbari (2016) and Alzabeebee et al. (2017) studied the behaviour of buried flexible pipes under static surface loads. Lay and Brachman (2014), Rakitin and Xu (2014), MacDougall et al. (2016) and Alzabeebee et al. (2017, 2018a) investigated the behaviour and the design of buried concrete pipes under static surface loads. McGrath et al. (2002) reported the results of a field study on the response of a buried flexible pipe

subjected to moving truck loads with a maximum axle load of 107 kN. Li et al. (2017) investigated the response of a buried concrete pipe and a rectangular culvert under the effect of a moving aircraft wheel load using a two-dimensional finite element analysis. The wheel load was modelled as a strip load with a maximum stress of 1482 kPa. However, there was no justification with regard to the use of a strip load and a two-dimensional finite element method for modelling such a complicated three-dimensional problem. Finally, Neya et al. (2017) conducted a three-dimensional finite element study on the behaviour of a buried pressurized steel pipe under moving vehicle loads.

In summary, it cannot be conclusively established, based on the previous studies, if the static or moving load should be used to study the behaviour of buried pipes and, hence for the design of buried pipes. Therefore, this study aimed to find the critical traffic loading condition on buried pipes by:

1- Developing and validating robust finite element models for simulating the behaviour of buried pipes under static and moving traffic loads.
2- Investigating the effect of truck speed and pipe stiffness on the maximum pipe displacement.
3- Investigating the effect of the truck speed and pipe stiffness on the ratio of the pipe displacement due to static traffic loads to the pipe displacement due to moving traffic loads.

The following section discusses the methodology of the finite element modelling.

2. Finite element model development

This section discusses the development and the validation of the methodology of the dynamic and static finite element analyses. Six case studies have been used to validate the models. These case studies were considered to develop a robust finite element model able to accurately simulate the behaviour of buried culverts under both static and moving loads with different loading configurations, and with different speeds of moving loads.

2.1. Modelling of buried pipes under moving loads

This section presents the development of the finite element model for buried pipes under moving loads using five case studies available in the literature (Mellat et al., 2014; Sheldon et al., 2015).

2.1.1. Validation problem 1

Mellat et al. (2014) investigated the displacement of a buried, in-service, large diameter, corrugated culvert under moving train loads using field and finite element studies. An X52 commuter train with a speed of 180 km/h was used in the field test. The culvert had an elliptical cross section. The horizontal dimension of the culvert was 3.75 m, while the vertical dimension was 4.15 m. The total length of the train was 54 m and consisted of two coaches. Each coach had four axles with a total axle load of 185 kN. The distance between the axles is shown in Figure 1. The finite element analysis involved modelling the field test using ABAQUS software, where linear elastic modelling was considered in the finite element analysis.

This study was considered because all of the information required for conducting the correct modelling (i.e. material properties of the culvert and the soil, culvert dimensions and loading configurations) are available in Mellat et al. (2014). In addition, the test was also modelled by Mellat et al. (2014) using ABAQUS software, as mentioned in the previous paragraph; hence, this allowed a direct comparison between the numerical modelling results of MIDAS GTS/NX (the finite element software used in this study) and ABAQUS.

The problem was modelled using the dimensions for the field dimensions as provided in Mellat et al. (2014). The corrugated culvert was simulated by using shell elements with an equivalent thickness of 0.061 m as proposed by Mellat et al. (2014). Four noded tetrahedron solid elements were used to model the ballast and the backfill layers; while three noded triangular shell elements were used to model the culvert. The base of the model was restrained against movement in all directions; while the sides of the model were restrained against movement in the horizontal direction. Ground surface spring elements (viscous dampers) were used in the sides and the bottom of the model to model the infinite boundary conditions. This

technique is used to eliminate the effect of S and P wave reflection (Sayeed and Shahin, 2016; Sayeed and Shahin, 2017). The damper properties with respect to the P wave (***DPW***) and S wave (***DSW***) are calculated automatically in MIDAS GTS/NX using Equations 1 and 2, respectively (MIDAS IT. Co. Ltd., 2015).

$$DPW = \rho \times A \times \sqrt{\frac{\lambda + 2 \times G}{\rho}} \quad (1)$$

$$DSW = \rho \times A \times \sqrt{\frac{G}{\rho}} \quad (2)$$

$$\lambda = \frac{\upsilon \times E}{(1 + \upsilon) \times (1 - 2 \times \upsilon)} \quad (3)$$

$$G = \frac{E}{2 \times (1 + \upsilon)} \quad (4)$$

Where, DPW is the damper properties with respect to the P wave, DSW is the damper properties with respect to the S wave, $\boldsymbol{\rho}$ is the density of the soil, A is the cross-section area, E is the modulus of elasticity of the soil and υ is the Poisson's ratio of the soil (MIDAS IT. Co. Ltd., 2015).

The finite element model was developed with an average element size of 0.25 m, 0.5 m and 0.5 m for the ballast layer, culvert, and the backfill and surrounding soil, respectively. A rough interaction (i.e. no interface element) between the soil and the culvert has been considered in the analysis. This is valid because the displacement inducted in the culvert is very small and hence, the slippage between the soil and the culvert will have an insignificant effect on the accuracy of the developed model (Xu et al., 2017; Alzabeebee et al., 2018b). The mesh of the developed three-dimensional finite element model is shown in Figure 2.

The moving wheels were modelled as concentrated moving loads using a train dynamic load table available in MIDAS GTS/NX. This modelling technique allows the user to model moving loads by specifying the nodes of the loading path and arranging a table for the wheel loads, the offset distance between the wheels and the train speed. By using this technique, the program automatically changes the loads on the mesh as the time increases, depending on the speed of the train. The

194 program also assumes that for each point load, the load distributes in a triangular
195 fashion among three nodes as shown in Figure 3 (Araújo, 2011; Sayeed and Shahin,
196 2016). The program also calculates the location of the maximum load based on the
197 train speed. It should be noted that the moving wheels were modelled as
198 concentrated loads because the wheel load concentrates below the rail seat and
199 does not distribute equally on the whole sleeper area due to the issues associated
200 with the contact area between the sleeper and the ballast layer as noted by Shenton
201 (1978) and Abadi et al., (2015). Hence, using point loads to model the moving train
202 loads does not affect the accuracy of the finite element model predictions.

203 A time step (Δt) of 0.004 sec was considered in the analysis based on the finite
204 element mesh size and the speed of the train following the Courant-Friedrichs-Lewy
205 condition (Galavi and Brinkgreve, 2014) using Equation 5. The time step was
206 calculated based on the mesh size to avoid the model instability caused by the wave
207 progress in the dynamic finite element analysis (Vivek, 2011). The material
208 properties of the ballast, backfill and culvert were taken from Mellat et al. (2014) and
209 are shown in Table 1.

$$\Delta t = \frac{C_n \times L_{min}}{V} \tag{5}$$

210 Where, C_n is the Courant number; L_{min} is the distance between two neighbouring
211 nodes on the path of the moving load; and V is the speed of the moving load (i.e.
212 speed of the train/truck).

213 The measured (field) results, numerical results using ABAQUS (Mellat et al. 2014)
214 and the numerical results from the present analysis (using MIDAS GTS/NX) for the
215 culvert crown displacement induced due to a moving X52 train with a speed of 180
216 km/h are shown in Figure 4. It is worth mentioning that Mellat et al. (2014) did not
217 model all of the train loads in their finite element analysis; they considered only the
218 two middle bogie loads of the train to reduce the computational time. It can be seen
219 from Figure 4 that the developed model predicts the crown displacement with very
220 good accuracy compared to the field data and ABAQUS analysis results. The
221 maximum displacement is 0.33 mm compared to a recorded value of 0.35 mm
222 (percentage difference is 6%). Furthermore, the developed model is able to predict

the trend of the displacement time relationship, as can be clearly seen in Figure 4. Hence, these observations give confidence in the methodology adopted for modelling this complex problem. Therefore, the developed model can be taken forward to investigate other scenarios of buried culverts under traffic loading.

Table 1: Material properties for the soil and the culvert (Mellat et al. 2014)

Material	E (kPa)	υ	γ (kN/m^3)
Ballast	200,000	0.3	17.65
Backfill and surrounding soil	100,000	0.3	15.7
Culvert	23,700,000	0.3	76.52

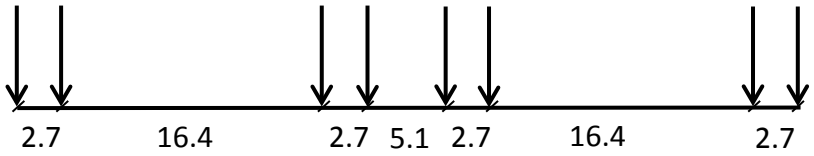

Figure 1: The distances between the axles of the X52 train (Mellat et al. 2014) (Note: all dimensions are in m)

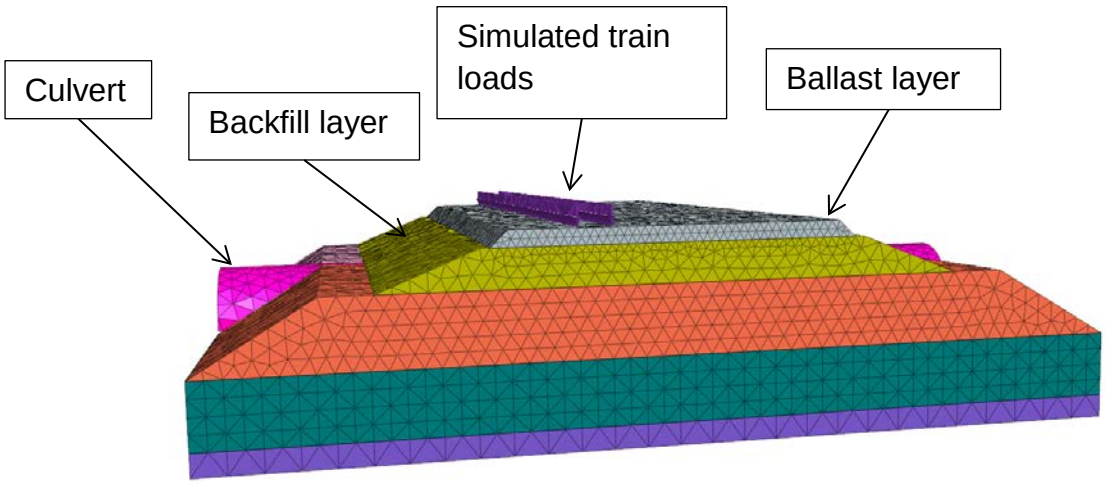

Figure 2: The finite element mesh used for validation problem 1

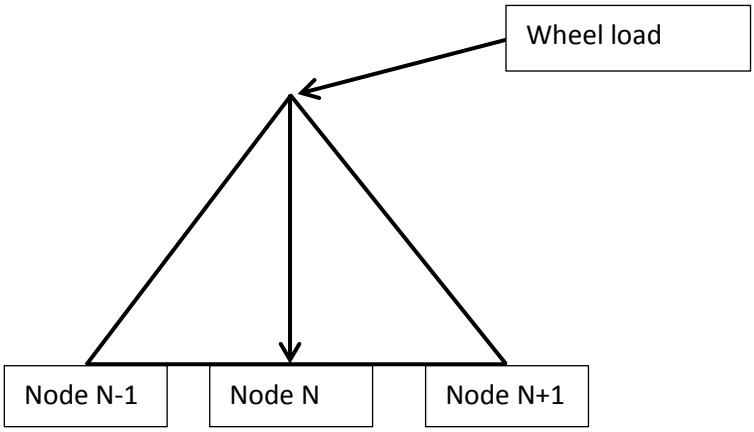

Figure 3: The assumption of moving load distribution (Araújo, 2011; Sayeed and Shahin, 2016)

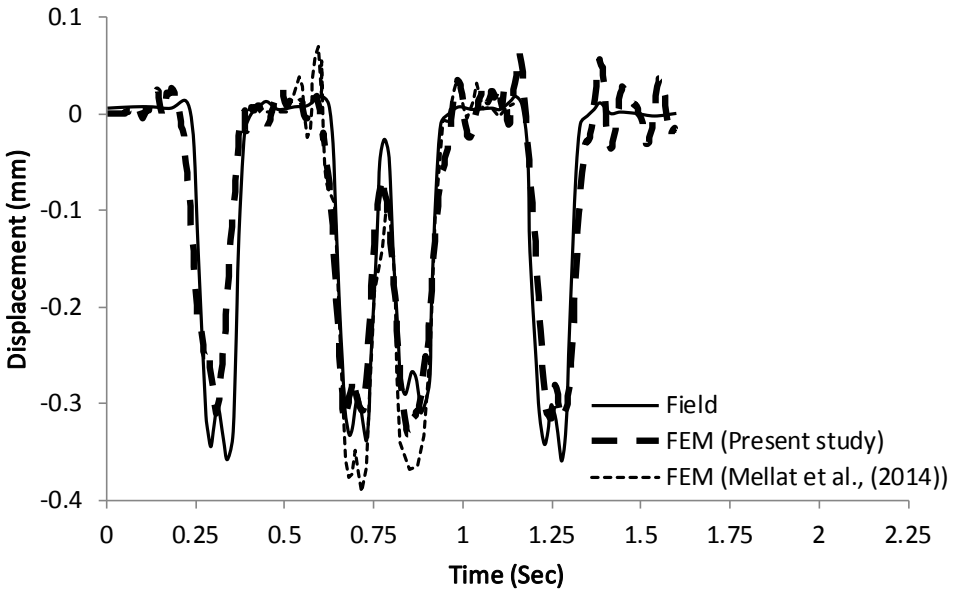

Figure 4: Crown displacement versus time response due to the effect of moving loads

2.1.2. Validation problem 2

Sheldon et al. (2015) reported the displacement response of a buried, in-service, corrugated metal pipe under the effect of static and moving truck loads. The moving truck tests were carried out at four different speeds (8 km/h, 16 km/h, 32 km/h and 48 km/h). The pipe had an inner diameter of 1.2 m and was buried with a backfill

height of 0.54 m. Linear displacement sensors were used to measure the crown displacement. These sensors were installed in the upstream and downstream sides of the pipe joint. The upstream sensor recorded the vertical displacement of the pipe crown and the downstream sensor recorded the vertical displacement of the pipe joint. The test truck had a steering axle load of 59 kN and rear axle load of 133 kN. The axles were spaced at 4.3 m. The distance between the rear wheel pairs was equal to 1.4 m.

These tests have been modelled using MIDAS GTS/NX to provide additional confidence in the methodology of the dynamic finite element analysis. In addition, the results have been compared to the results using static loads, as will be discussed in section 2.2.

Four noded tetrahedron solid elements were used to model the soil and the asphalt layer; while three noded triangular shell elements were used to model the pipe. The joint was not considered in the finite element model as the aim was to model the behaviour of the buried pipe under static and moving loads to test the finite element analysis methodology. The model had a width, length and height of 5 m, 15 m and 10 m, respectively. A trench with a width of 2.4 m, a height of 2.14 m and a length of 15 m was considered in the model to enable finer elements to be used around the pipe to improve the prediction accuracy. The model was built with an average element size of 0.15 m for the pipe, 0.15 m for the trench, 0.25 m for the road and 0.5 m for the natural soil. A rough interaction (i.e. no interface element) between the soil and the pipe has been considered in the analysis. The pipe was modelled using an effective thickness of 0.0165 mm; this value has been calculated by Sheldon (2011). The three-dimensional finite element model is shown in Figure 5. The base of the model was restrained against movement in all directions, while the sides of the model were restrained against movement in the horizontal direction. Ground surface spring elements were used in the sides and the bottom of the model to simulate infinite boundaries.

A well graded sandy soil with a degree of compaction of 90% (SW90) was considered in the model as a backfill soil, followed by an asphalt layer with a thickness of 0.1 m. A linear elastic model was used to simulate the behaviour of the pavement and pipe as the applied load was below the yield stress of both the asphalt

and the pipe material. However, the soil was modelled using the linear elastic model (LE) and the Mohr-Coulomb elastic perfectly plastic model (MC) to study the effect of including the soil plasticity on the accuracy of the predictions of the finite element model. The modulus of elasticity (E) of the SW90 soil was calculated using Equation 6 (Janbu, 1963) utilising the hyperbolic soil model parameters (K = 950 and n = 0.60) published by Boscardin et al. (1990). These hyperbolic parameters were determined from triaxial test results (further information can be found in Boscardin et al., 1990). A lateral stress (S_3) of 19.32 kPa was used in Equation 6 to calculate the modulus of elasticity. This lateral stress was calculated by taking the average height from the top surface of the model to the pipe invert using a coefficient of lateral earth pressure of 1.0 for the compacted backfill soil (Brown and Selig, 1991) (i.e.$(1.74 \times 21 \times 1)/2$). The average height to the pipe invert has been considered in the analyses because the behaviour of the pipe is significantly affected by the support condition provided at the pipe springline and the pipe invert (Dhar et al., 2004). The natural soil was assumed to be stronger than the backfill soil (K = 1500 and n = 0.65) (Alzabeebee et al., 2017). The material properties of the SW90 soil, the natural soil, the asphalt layer and the pipe are taken from the literature (Boscardin et al. 1990; Kang et al., 2014; Sheldon et al., 2015; Alzabeebee et al., 2017) and are shown in Table 2. It should be noted that the pipe tested by Sheldon et al. (2015) was an in-service buried culvert. Hence, the backfill soil around the pipe was very compacted due to the repeated action of moving trucks and cars. Hence, the use of a very compacted soil (SW95) in the modelling of the backfill soil was deemed most appropriate. In addition, the parameters considered for the culvert are the real parameters of the pipe material based on Sheldon (2011). On the other hand, the parameters for the asphalt and the surrounding soil have been considered from other references due to the lack of information in the original references (i.e. Sheldon (2011) and Sheldon et al. (2015)).

$$E = K \times P_a \times \left(\frac{S_3}{P_a}\right)^n \quad (6)$$

Where, E is the modulus of elasticity of the soil; K and n are the hyperbolic parameters for the stiffness modulus; P_a is the atmospheric pressure (100 kPa); and S_3 is the lateral stress.

The moving truck loads were modelled, assuming concentrated moving loads, with the aid of the dynamic train table available in the MIDAS GTS/NX software as discussed in validation problem 1. The truck tyres were modelled as concentrated moving loads because the load applied by the moving tyre concentres and does not distribute uniformly on the whole tyre contact area as noticed by De Beer et al. (1997) and the tyre contract stress has not been measured during the tests. Furthermore, Shakiba et al. (2017) noticed that using non-uniform complex loads in modelling the effect of the moving loads affects the accuracy of the finite element modelling only at shallow depths in comparison with the concentrated loads, where the differences between non-uniform and concentrated loads diminish at the bottom of the asphalt layer. Hence, the assumption of the concentrated load was considered valid as the considered pipe is buried with a backfill height of 0.45 m. The space between the concentrated loads was considered equal to 1.4 m, similar to that reported in the field tests. The time step (Δt) was calculated based on the mesh size and the velocity of the truck following the Courant-Friedrichs-Lewy condition (Galavi and Brinkgreve, 2014) using Equation 5.

The measured and predicted crown displacement time response of the pipe under moving trucks with speeds of 8 km/h, 16 km/h, 36 km/h and 48 km/h are shown in Figures 6, 7, 8 and 9, respectively. It can be seen that the developed model is able to predict the trend behaviour of the displacement time response for all of the considered speeds. However, Figures 6 and 7 show a shift in the results of the finite element simulation in comparison with the field tests. This might be due to issues related to a change in the truck speed during the tests. Importantly, the developed model predicted the maximum displacement with very good accuracy, where the percentage difference of the field and numerical maximum crown displacements are equal to 3%, 5%, 22% and 20% for truck speeds of 8 km/h, 16 km/h, 32 km/h and 48 km/h, respectively. Furthermore, the difference in the results can also be justified by the potential variability in the test results, especially for such complicated field tests and the uncertainties associated with such tests. Figures 6, 7, 8 and 9 also show that the LE and the MC models give the same displacement, illustrating the insignificant effect of including the soil plasticity on the results (i.e. pipe behaviour). This occurred because the soil around the pipe did not reach the condition of failure due to the applied surface pressure. Hence, the support condition provided to the pipe in the

MC analysis was similar to that provided with the LE analysis. This observation is consistent with that reported by Robert et al. (2016) and Katona et al. (2017). Therefore, it can be concluded that the linear elastic model can be used to predict the behaviour of buried pipes under paved roads with a good accuracy.

Table 2: Material properties used in the finite element analysis

Property	Natural soil*	Backfill soil**	Asphalt***	Pipe****
γ (kN/m^3)	21.00	21.00	23.23	78.00
υ	0.3	0.3	0.3	0.2
E (kPa)	49,685	30,813	4,500,000	200,000,000
c'(kPa)	30	1	---	---
ϕ'(°)	36	48	---	---

* adopted from Alzabeebee et al. (2017); ** adopted from Boscardin et al. (1990) and the modulus of elasticity calcualted using Equation 6; *** adopted from Kang et al. (2014); **** adopted from Sheldon et al. (2015).

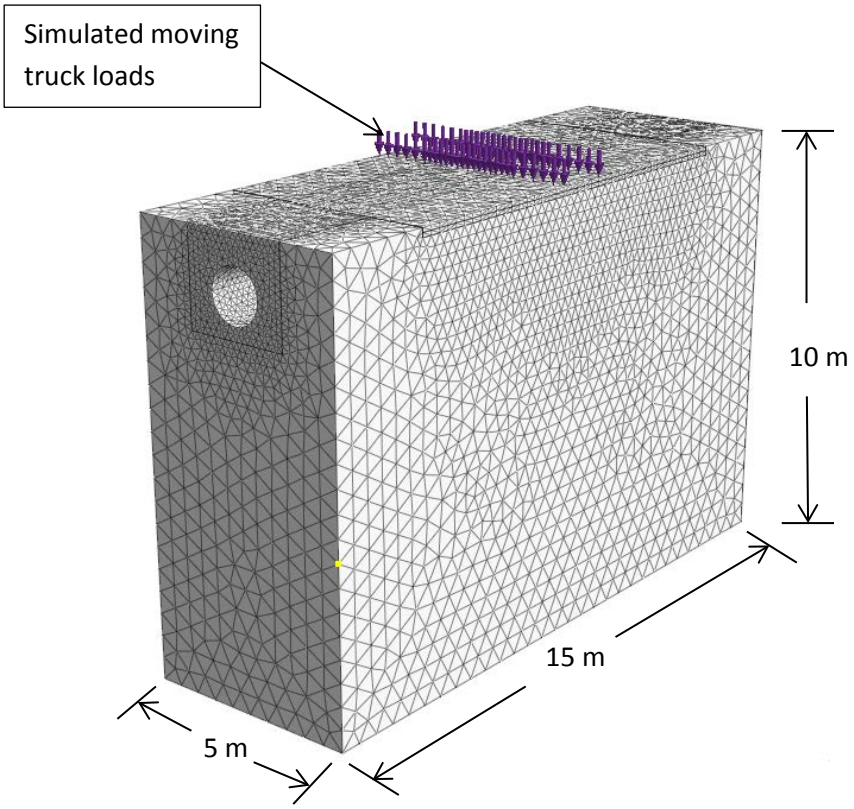

Figure 5: The finite element mesh used for validation problem 2

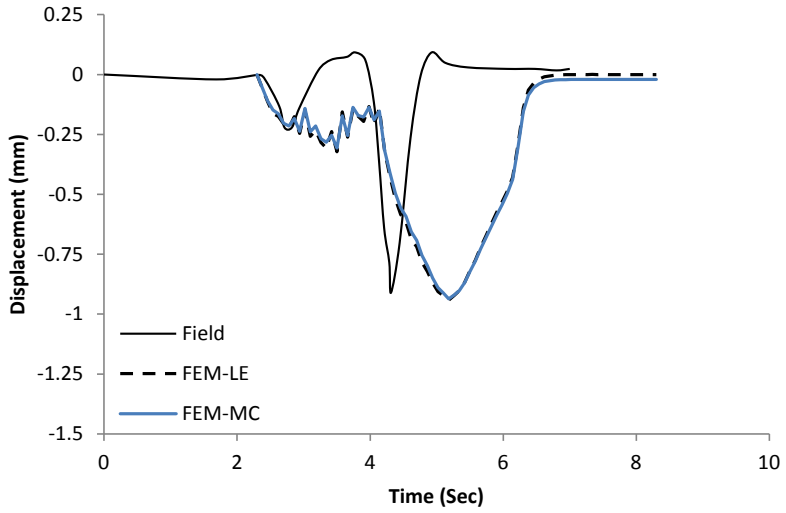

359

360 Figure 6: Crown displacement time response under a moving truck with a speed of 8
361 km/h

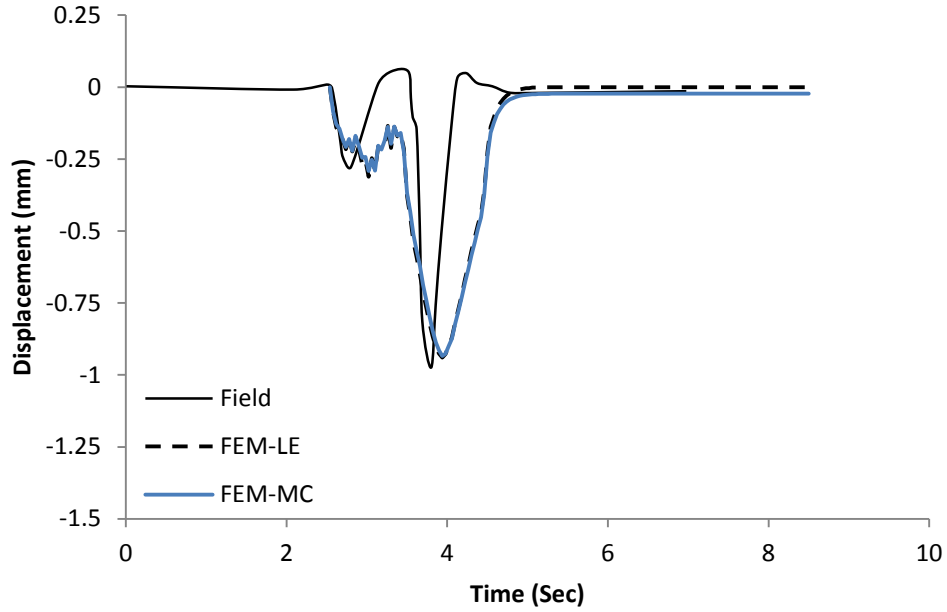

362

363 Figure 7: Crown displacement time response under a moving truck with a speed of
364 16 km/h

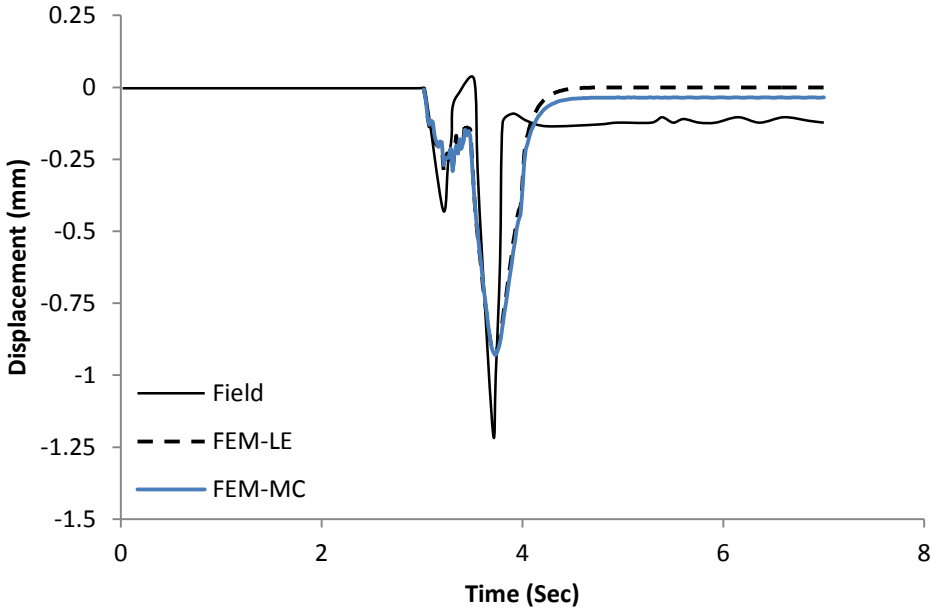

365

366 Figure 8: Crown displacement time response under a moving truck with a speed of
367 32 km/h

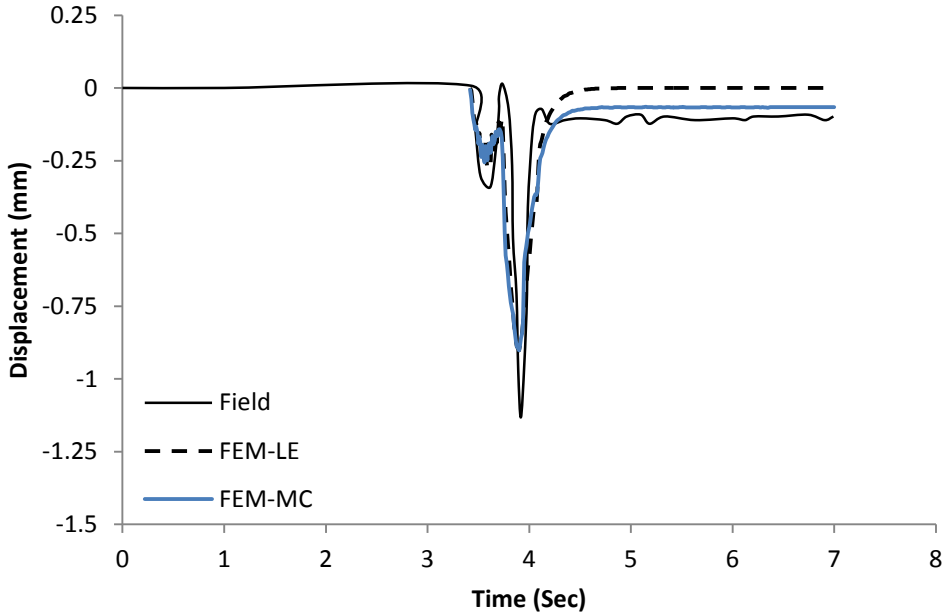

368

369 Figure 9: Crown displacement time response under a moving truck with a speed of
370 48 km/h

2.2. Modelling buried pipes under static loads

Another finite element model for buried pipes under static loads has been developed and validated in this section to study the behaviour of the metal pipe (modelled in validation problem 2) under static loads and to compare the behaviour under static and dynamic moving loads. The case of the rear axle being directly on the top of the pipe was considered as Sheldon et al. (2015) found that this loading condition created the worst-case scenario. The static loads were applied in one increment because the linear elastic static analysis does not require the load to be applied in steps. The tyre load was modelled as a surface pressure over a tyre foot print area of approximately 0.25 m x 0.50 m (Sheldon, 2011); as this technique was found to provide a good prediction to the response of the buried pipes under static loads (Yeau et al., 2014; Alzabeebee et al., 2017, 2018a, b). The obtained maximum static displacement of the crown of the buried pipe was equal to 1.28 mm, compared to an experimental value of 1.49 mm, indicating a good predictive ability for the developed model.

Figure 10 shows the ratio of the maximum predicted static crown displacement (1.28 mm) to the maximum predicted dynamic crown displacement (pipe displacement due to the moving traffic loads predicted form the finite element model) for different truck speeds (obtained from Figures 6, 7, 8 and 9). It can be clearly seen from the Figure 10 that the static displacement is higher than the dynamic displacement for all of the truck speeds, where the ratio ranges from 1.36 to 1.42 depending on the truck speed. This is similar to the observations reported by Yeau et al. (2009). In addition, Figure 10 also shows the same ratio (i.e. the maximum static crown displacement to the maximum dynamic crown displacement) calculated based on the results from Sheldon et al. (2015). It can be seen that the ratio based on the results from Sheldon et al. (2015) show some differences from those predicted based on the finite element modelling. The ratio increases with the increase of the truck speed up to 8 km/hr, then decreases as the speed increases from 8 km/hr to 32 km/hr. Finally, the ratio increases again as the speed changes from 32 km/hr to 48 km/hr. These differences may be due to the potential variability in the test results, especially for such complicated field tests and the uncertainties associated with such tests as discussed in Section 2.1.2. In addition, the relative magnitudes of the static and dynamic

displacement are very small (less than 1.25 mm), and hence a small difference/inaccuracy could produce a large variation in the ratio.

It can also be seen in Figure 10 that there is a drop in the ratio as the truck changes from moving to static (i.e. speed = 0 km/hr). This is due to the significant difference of the stress distribution caused by the moving load action as demonstrated by De Beer et al. (1997). On the other hand, the load distributes uniformly for the static load case. The drop in the ratio has also been noted by Yea et al. (2009) and Sheldon et al. (2015).

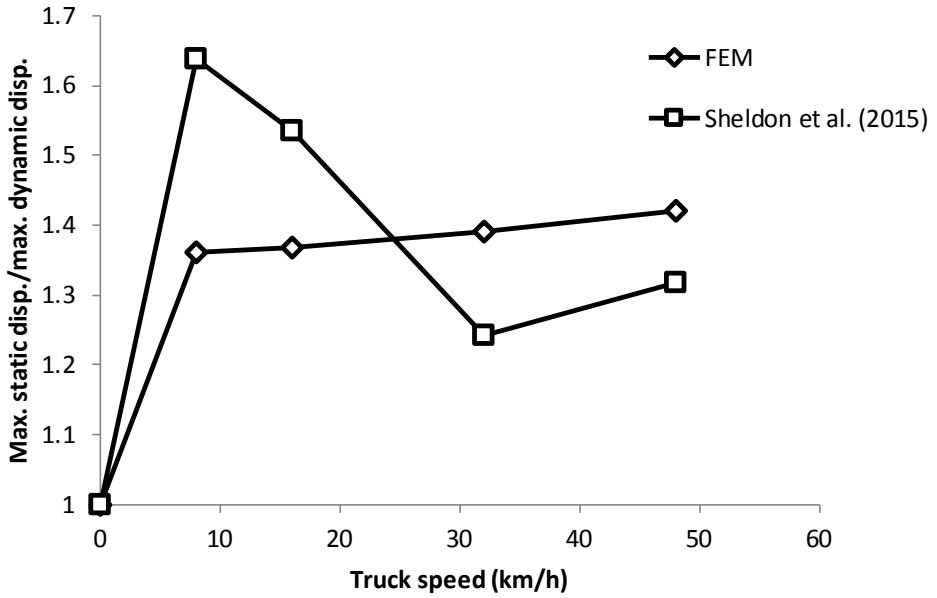

Figure 10: Ratio of the maximum static displacement to the maximum dynamic displacement for different truck speeds for a buried metal pipe

3. Parametric study

A parametric study has been carried out to study the effect of the truck speed and pipe stiffness (PS) on the maximum pipe displacement and the ratio of the static to dynamic maximum pipe displacement. This was considered because the behaviour of the buried pipe is significantly affected by the pipe stiffness based on the arching mechanism (Moore, 2001; Kang et al., 2007). In addition, increasing the pipe stiffness decreases the response of the buried pipe to the applied loads. Therefore, it was important to conduct this investigation before recommending the use of the

static load in future pipe studies. A truck speed ranging from 8 km/hr to 76 km/hr was considered in the analyses. The pipe stiffness was calculated using Equation 7 (Petersen et al., 2010). Four values of pipe stiffness were considered in the analysis (0.5 kN/m, 10 kN/m, 102 kN/m and 1022 kN/m). These values cover the range of very flexible, flexible, semi-rigid and rigid pipes (Bryden et al., 2015). The diameter for all of these pipes was kept constant (1.2 m), i.e. similar to the diameter of the metal pipe used in the validation problem, while the thickness was assumed to be equal to 0.08 m. However, the modulus of elasticity was changed to alter the pipe stiffness based on Equation 7. The truck used in the analyses had a loading configuration to the same as that used in the study of Sheldon et al. (2015) (i.e. the truck used in Validation problem 2).

$$PS = \frac{EI}{0.149\, r^3} \tag{7}$$

Where, E is the modulus of elasticity of the pipe; I is the moment of inertia of the pipe; and r is the mean radius of the pipe.

Figures 11, 12, 13 and 14 show the crown displacement against time response due to the effect of moving traffic loads for very flexible, flexible, semi-rigid and rigid pipes, respectively. The figures show that the trend of the crown displacement with time is similar for all the pipes. In addition, the figures also show that increasing truck speed slightly decreases the induced maximum pipe crown displacement. Increasing the truck speed from 8 km/hr to 76 km/hr decreases the maximum pipe crown displacement by 6%, 7%, 8% and 9% for very flexible, flexible, semi-rigid and rigid pipes, respectively. In addition, the results show that increasing the pipe stiffness decreases the crown displacement. This behaviour is due to the decrease in the response of the buried pipe to the applied load as the pipe stiffness increases (Alzabeebee et al., 2017).

Figure 15 shows the relationship between the ratio of the static to dynamic maximum pipe displacement and truck speed for different values of pipe stiffness. It can be seen from the figure that the static pipe displacement is always higher than the dynamic pipe displacement (i.e. the ratio is higher than 1) for all of the considered values of pipe stiffness. In addition, the figure shows that the ratio of the static to

dynamic pipe displacement slightly increases as the truck speed increases. This behaviour is due to the slight decrease in the maximum dynamic pipe displacement as the truck speed increases. Furthermore, the figure shows that increasing the pipe stiffness significantly decreases the ratio of the static to dynamic pipe displacement. For example, for a truck speed of 8 km/hr and 76 km/hr, the ratio of the static to dynamic pipe displacement decreases by 34% and 33%, respectively, as the stiffness of the pipe changes from 0.5 kN/m to 1022 kN/m (i.e. the pipe changes form very flexible to rigid).

In summary, the results of the parametric study clearly illustrate that the static load represents the worst-case scenario in all the cases considered in this study. Therefore, the static load should be used in the analysis and the design of buried pipes.

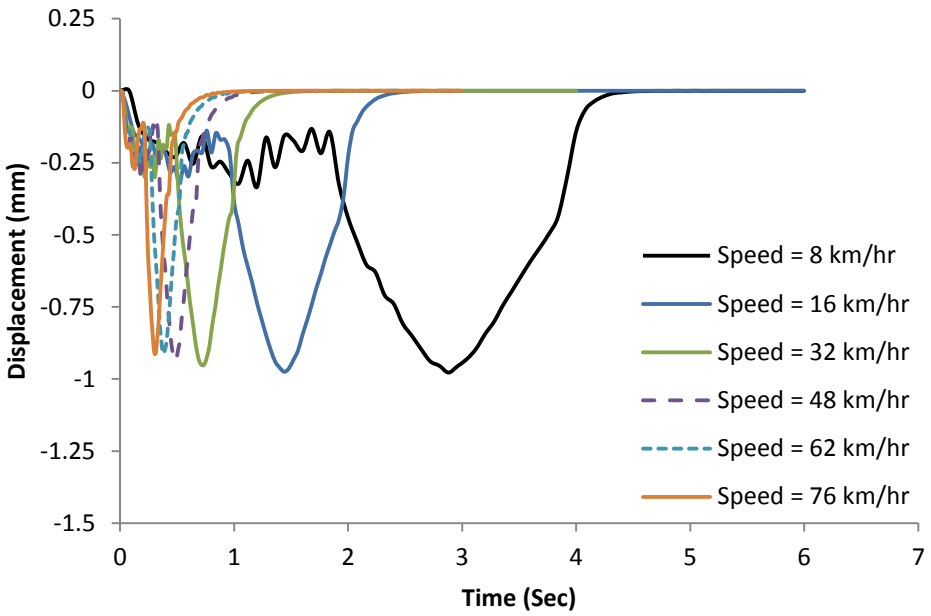

Figure 11: Crown displacement versus time response under a moving truck with different truck speeds for a very flexible pipe ($PS = 0.5\ kN/m$)

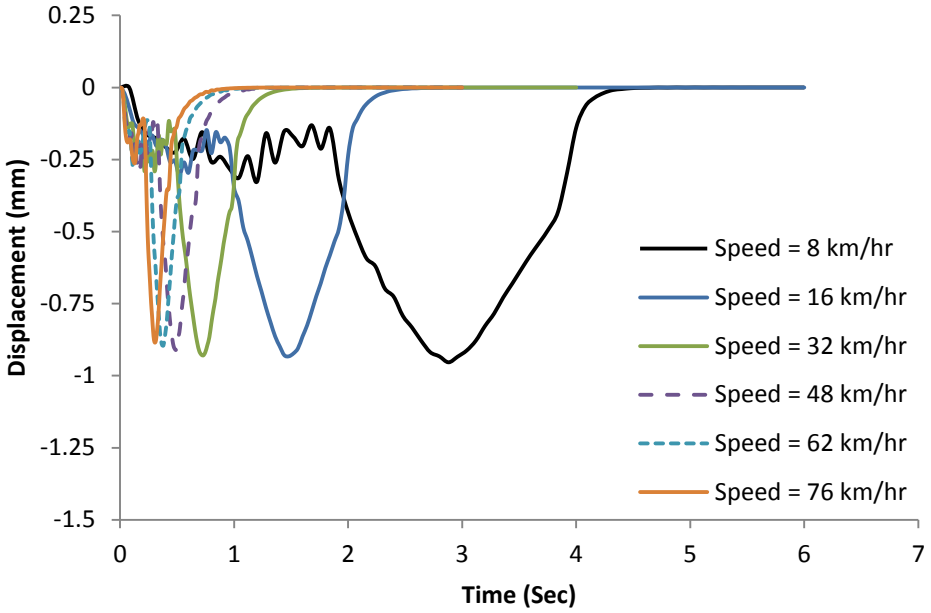

467

468 Figure 12: Crown displacement versus time response under a moving truck with
469 different truck speeds for a flexible pipe ($PS = 10\ kN/m$)

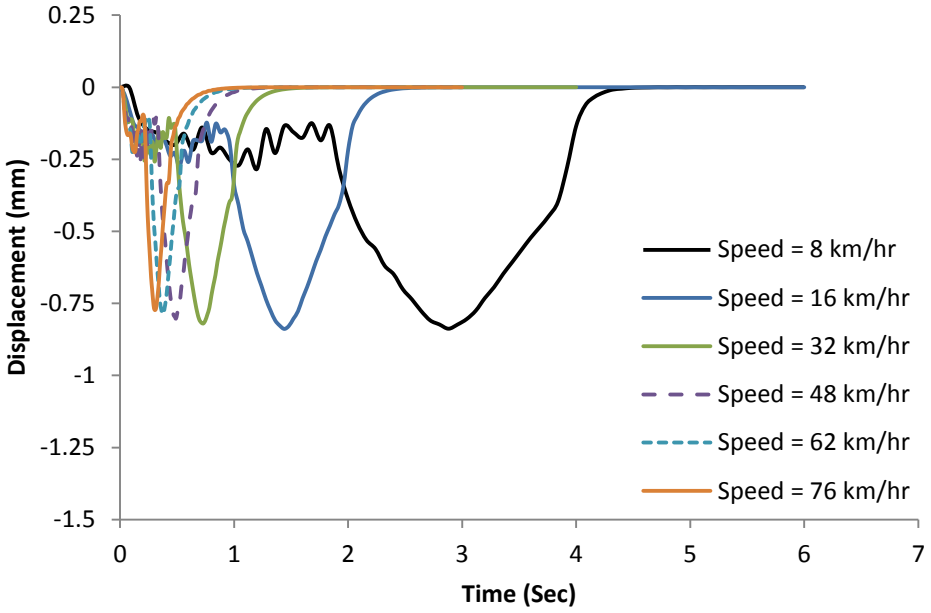

470

471 Figure 13: Crown displacement versus time response under a moving truck with
472 different truck speeds for a semi-rigid pipe ($PS = 102\ kN/m$)

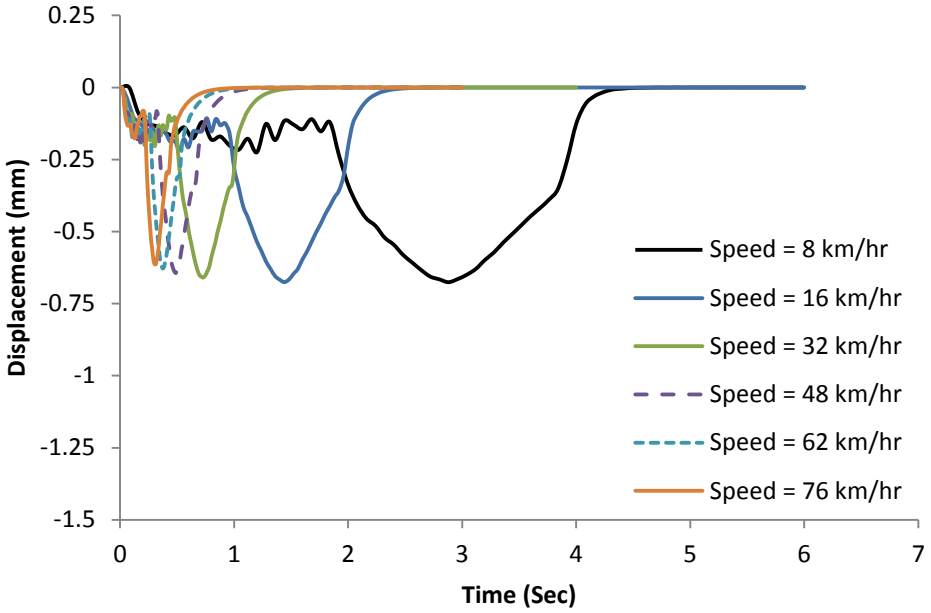

473

474 Figure 14: Crown displacement versus time response under a moving truck with
475 different truck speeds for a rigid pipe ($PS = 1022\ kN/m$)

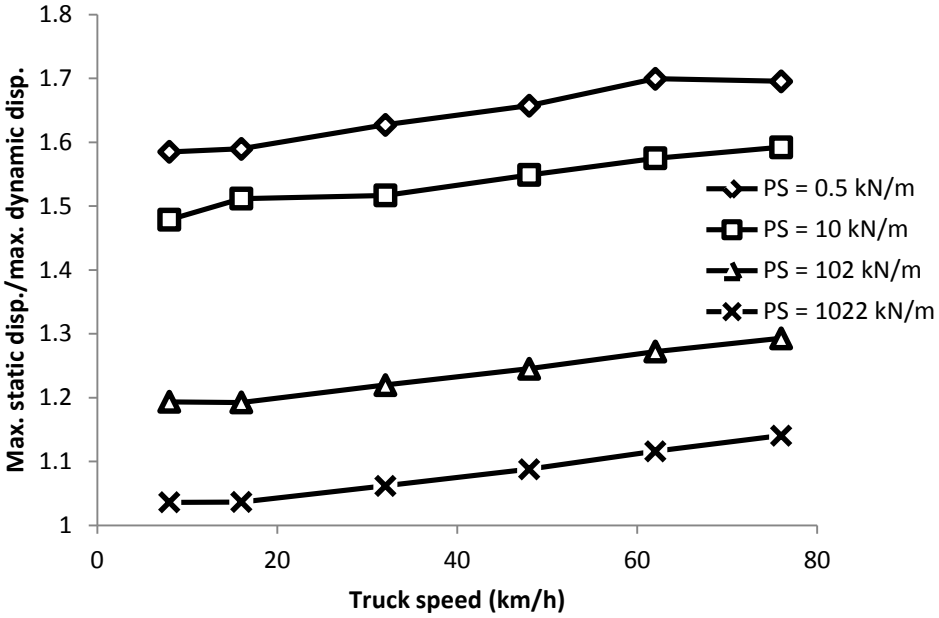

476

477 Figure 15: Effect of the pipe stiffness on the static to dynamic pipe displacement for
478 different truck speeds

4. Summary and conclusions

This paper has compared the behaviour of buried pipes under both static and moving traffic loads to find the critical loading condition which should be used in the analysis and the design of buried pipes. The study was conducted using rigorous finite element analyses. The methodology of the dynamic and static finite element analysis was validated using six case studies available in the literature. A parametric study was then conducted to study the effect of the truck speed and pipe stiffness on the induced maximum pipe crown displacement. In addition, the ratio of the static to dynamic pipe crown displacement was also investigated. The following conclusions can be drawn based on the findings from this study:

1- Including the soil plasticity does not affect the accuracy of the finite element analysis of buried pipes under paved roads. Hence, linear elastic analyses can be used to simulate the behaviour of buried pipes under a paved road with a backfill height equal to or more than 0.45 m and subjected to static and moving traffic loads with a maximum axle load of 133 kN. The percentage difference of the finite element analyses and the field tests results ranged from 3% to 20%, indicating a good prediction from the finite element models, given the assumptions made in the numerical analyses and the uncertainties associated with complicated field tests.

2- Simulating the moving traffic loads using concentrated loads produced very good agreement with the field results. This finding confirms the observation of De Beer et al. (1997), who noted that the forces transmitted from the moving wheel to the pavement tend to concentrate and do not distribute uniformly over all of the wheel contact area.

3- Increasing the truck speed caused a small decrease in the induced maximum pipe crown displacement. The percentage decrease was 6%, 7%, 8% and 9% for very flexible, flexible, semi-rigid and rigid pipes, respectively, as the truck speed changed from 8 km/hr to 76 km/hr.

4- The static traffic loads produced a deformation higher than the moving traffic loads for all of the pipes considered in this study. The ratio of the static to dynamic maximum pipe displacement ranged between 1.04 to 1.70 depending on the pipe stiffness and the truck speed. Hence, future studies

should consider the static loading condition to simulate the worst-case scenario.

5- The ratio of the static to the dynamic pipe crown displacement decreases with an increase in pipe stiffness.

Acknowledgment

The first author thanks the financial support for his PhD study provided by the higher committee for education development in Iraq (HCED).

References

Abadi, T., Le Pen, L., Zervos, A. and Powrie, W., 2015. Measuring the area and number of ballast particle contacts at sleeper/ballast and ballast/subgrade interfaces. International Journal of Railway Technology, 4(2), 45-72.

Acharya, R., Han, J., Brennan, J.J., Parsons, R.L. and Khatri, D.K., 2016. Structural response of a low-fill box culvert under static and traffic loading. Journal of Performance of Constructed Facilities, 30(1), 04014184.

Alzabeebee, S., 2017. Enhanced design approaches for rigid and flexible buried pipes using advanced numerical modelling. PhD thesis, the University of Birmingham.

Alzabeebee, S., Chapman, D., Jefferson, I. and Faramarzi, A., 2017. The response of buried pipes to UK standard traffic loading. Proceedings of the Institution of Civil Engineers - Geotechnical Engineering 170(1), 38-50.

Alzabeebee, S., Chapman, D. and Faramarzi, A., 2018a. Economical design of buried concrete pipes subjected to UK standard traffic loading. Proceedings of the Institution of Civil Engineers – Structures and Buildings, https://doi.org/10.1680/jstbu.17.00035.

Alzabeebee, S., Chapman, D.N. and Faramarzi, A., 2018b. Development of a novel model to estimate bedding factors to ensure the economic and robust design of rigid pipes under soil loads. Tunnelling and Underground Space Technology 71, 567-578.

Araújo, N.M.F., 2011. High-speed trains on ballasted railway track: dynamic stress field analysis, PhD thesis, University of Minho.

Arockiasamy, M., Chaallal, O. and Limpeteeprakarn, T., 2006. Full-scale field tests on flexible pipes under live load application. Journal of Performance of Constructed Facilities 20(1), 21–27.

Beben, D., 2013. Dynamic amplification factors of corrugated steel plate culverts. Engineering Structures, 46, 193-204.

Boscardin, M.D., Selig, E.T., Lin, R.S. and Yang, G.R., 1990. Hyperbolic parameters for compacted soils. Journal of Geotechnical Engineering ASCE, 116(1): 88-104.

Brown, S.F. and Selig, E.T., 1991. “The design of pavement and rail track foundations.” In O’Reilly, M. P. and Brown, S. F. (eds.) Cyclic loading of soils: from theory to practice. Glasgow and London: Blackie and Son Ltd. pp. 249-305.

Bryden, P., El Naggar, H. and Valsangkar, A., 2015. Soil-structure interaction of very flexible pipes: centrifuge and numerical investigations. International Journal of Geomechanics, 15(6): 04014091.

Chaallal, O., Arockiasamy, M. and Godat, A., 2015a. Field test performance of buried flexible pipes under live truck loads. Journal of Performance of Constructed Facilities 29(5), 04014124.

Chaallal, O., Arockiasamy, M. and Godat, A., 2015b. Numerical finite-element investigation of the parameters influencing the behavior of flexible pipes for pipes and storm sewers under truck load. Journal of Pipeline Systems Engineering and Practice 6(2), 04014015.

De Beer, M., Fisher, C. and Jooste, F.J., 1997. Determination of pneumatic tyre/pavement interface contact stresses under moving loads and some effects on pavements with thin asphalt surfacing layers. In 8th International Conference on Asphalt Pavements. Seattle: pp.179-227. (Volume 1)

564 Dhar, A.S., Moore, I.D. and McGrath, T.J., 2004. Two-dimensional analyses of
565 thermoplastic culvert displacements and strains. Journal of Geotechnical and
566 Geoenvironmental Engineering, 130(2): 199-208.

567 Galavi, V. and Brinkgreve, R.B.J., 2014. Finite element modelling of geotechnical
568 structures subjected to moving loads. In: Hicks et al., editors. VIII ECNUMGE –
569 numerical methods in geotechnical engineering. Delft, Netherlands: Taylor & Francis
570 – Balkema. pp. 235-40.

571 Janbu, N., 1963. “Soil compressibility as determined by odometer and triaxial tests.”
572 In the European Conference on Soil Mechanics and Foundation Engineering.
573 Wiesbaden. Pp. 19-25 (Volume 1).

574 Kang, J., Parker, F. and Yoo, C.H., 2007. Soil-structure interaction and imperfect
575 trench installations for deeply buried concrete pipes. Journal of Geotechnical and
576 Geoenvironmental Engineering, 133(3): 277-285.

577 Kang, J., Stuart, S.J. and Davidson, J.S., 2014. Analytical study of minimum cover
578 required for thermoplastic pipes used in highway construction. Structure and
579 Infrastructure Engineering, 10(3): 316-327.

580 Katona M.G., 1990. Minimum cover heights for corrugated plastic pipe under vehicle
581 loading. Transportation Research Record: Journal of the Transportation Research
582 Board, 1288: 127-135.

583 Katona, M.G., 2017. Influence of soil models on structural performance of buried
584 culverts. International Journal of Geomechanics, 17(1): 04016031.

585 Khemis, A., Chaouche, A.H., Athmani, A. and Tee, K.F., 2016. Uncertainty effects of
586 soil and structural properties on the buckling of flexible pipes shallowly buried in
587 Winkler foundation. Structural Engineering and Mechanics, 59 (4), 739-759.

588 Lay, G.R. and Brachman, R.W.I., 2014. Full-scale physical testing of a buried
589 reinforced concrete pipe under axle load. Canadian Geotechnical Journal 51(4), 394-
590 408.

591 Li, Y., Song, G. and Cai, J., 2017. Mechanical response analysis of airport flexible
592 pavement above underground infrastructure under moving wheel load. Geotechnical
593 and Geological Engineering, 35(5), 2269-2275.

594 MacDougall, K., Hoult, N. A. and Moore, I.D., 2016. Measured load capacity of
595 buried reinforced concrete pipes. ACI Structural Journal, 113(1), 63-73.

596 McGrath, T.J., DelloRusso, S.J. and Boynton, J., 2002. Performance of
597 thermoplastic culvert pipe under highway vehicle loading. Pipelines2002: Beneath
598 Our Feet: Challenges and Solutions. ASCE, Cleveland, Ohio, USA, pp. 1-14.

599 Mellat, P., Andersson, A., Pettersson, L. and Karoumi, R., 2014. Dynamic behaviour
600 of a short span soil–steel composite bridge for high-speed railways–Field
601 measurements and FE-analysis. Engineering Structures, 69(15): 49-61.

602 MIDAS IT. Co. Ltd. Manual of GTS-NX 2015 v2.1: new experience of geotechnical
603 analysis system. South Korea: MIDAS Company Limited; 2015.

604 Mohamedzein, Y. and Al-Aghbari, M.Y., 2016. Experimental study of the
605 performance of plastic pipes buried in dune sand. International Journal of
606 Geotechnical Engineering, 10(3): 236-245.

607 Moore, I. D., 2001. Buried pipes and pipes. In Rowe, R. K. (ed.) Geotechnical and
608 Geoenvironmental Engineering Handbook. Norwell: Kluwer Academic Publishing.
609 pp. 539‑566.

610 Moser, A.P. and Folkman, S., 2008. Buried pipe design. 3rd ed. New York: The
611 McGraw-Hill.

612 Neya, B.N., Ardeshir, M.A., Delavar, A.A. and Bakhsh, M.Z.R., 2017. Three-
613 Dimensional Analysis of Buried Steel Pipes under Moving Loads. Open Journal of
614 Geology, 7: 1-11.

615 Petersen, D.L., Nelson, C.R., Li, G., McGrath, T.J. and Kitane, Y., 2010. NCHTP
616 Report 647: Recommended Design Specifications for Live Load Distribution to
617 Buried Structures. Transportation Research Board, Washington.

618 Rakitin, B. and Xu, M., 2014. Centrifuge modeling of large-diameter underground
619 pipes subjected to heavy traffic loads. Canadian Geotechnical Journal, 51(4), 353-
620 368.

621 Robert, D.J., Rajeev, P., Kodikara, J. and Rajani, B., 2016. Equation to predict
622 maximum pipe stress incorporating internal and external loadings on buried pipes.
623 Canadian Geotechnical Journal, 53(8): 1315-1331.

624 Sayeed, M.A. and Shahin, M.A., 2016. Three-dimensional numerical modelling of
625 ballasted railway track foundations for high-speed trains with special reference to
626 critical speed. Transportation Geotechnics, 6: 55-65.

627 Sayeed, M.A. and Shahin, M.A., 2017. Design of ballasted railway track foundations
628 using numerical modelling Part I: Development. Canadian Geotechnical Journal,
629 https://doi.org/10.1139/cgj-2016-0633.

630 Shakiba, M., Gamez, A., Al-Qadi, I.L. and Little, D.N., 2017. Introducing realistic tire–
631 pavement contact stresses into Pavement Analysis using Nonlinear Damage
632 Approach (PANDA). International Journal of Pavement Engineering, 18(11): 1027-
633 1038.

634 Sheldon, T., Sezen, H. and Moore, I.D., 2015. Joint response of existing pipe
635 culverts under surface live loads. Journal of Performance of Constructed
636 Facilities, 29(1): 04014037.

637 Sheldon, T.A., 2011. Beam-on-springs modeling of jointed culvert systems. MSc
638 thesis, The Ohio State University.

639 Shenton, M. J., 1978. Deformation of railway ballast under repeated loading
640 condition", in "Proceeding of Railroad Track Mechanics and Technology, Kerr, A.D,
641 (Editor), Princeton University, 1978.

642 Talesnick, M.L., Xia, H.W. and Moore, I.D., 2011. Earth pressure measurements on
643 buried HDPE pipe. Géotechnique, 61(9): 721-732.

644 Tee, K.F., Khan, L.R. and Chen, H.P., 2013. Probabilistic failure analysis of
645 underground flexible pipes. Structural Engineering and Mechanics, 47(2): 167-183.

646 Vivek, P., 2011. Static and dynamic interference of strip footings in layered soil.
647 M.Tech thesis. Indian Institute of Technology, Kanpur.

648 Xu, M., Shen, D. and Rakitin, B., 2017. The longitudinal response of buried large-
649 diameter reinforced concrete pipeline with gasketed bell-and-spigot joints subjected
650 to traffic loading. Tunnelling and Underground Space Technology, 64: 117-132.

651 Yeau, K.Y., Sezen, H. and Fox, P.J., 2009. Load performance of in situ corrugated
652 steel highway culverts. Journal of Performance of Constructed Facilities, 23(1): 32-
653 39.

654 Yeau, K.Y., Sezen, H. and Fox, P.J., 2014. Simulation of behavior of in-service metal
655 culverts. Journal of Pipeline Systems Engineering and Practice, 5(2): 04013016.

656 Zhou, M., Du, Y.J., Wang, F., Arulrajah, A. and Horpibulsuk, S., 2017. Earth
657 pressures on the trenched HDPE pipes in fine-grained soils during construction
658 phase: Full-scale field trial and finite element modeling. Transportation
659 Geotechnics, 12: 56-69.